

Spin-dependent sum rules connecting real and virtual Compton scattering verified

Vadim Lensky

*Institut für Kernphysik, Cluster of Excellence PRISMA,
Johannes Gutenberg Universität, Mainz D-55099, Germany*

Institute for Theoretical and Experimental Physics, 117218 Moscow, Russia and

National Research Nuclear University MEPhI (Moscow Engineering Physics Institute), 115409 Moscow, Russia

Vladimir Pascalutsa and Marc Vanderhaeghen

*Institut für Kernphysik, Cluster of Excellence PRISMA,
Johannes Gutenberg Universität, Mainz D-55099, Germany*

Chung Wen Kao

*Department of Physics and Center for High Energy Physics,
Chung-Yuan Christian University, Chung-Li 32023, Taiwan*

(Dated: November 6, 2018)

We present a detailed derivation of the two sum rules relating the spin polarizabilities measured in real, virtual, and doubly-virtual Compton scattering. For example, the polarizability δ_{LT} , accessed in inclusive electron scattering, is related to the spin polarizability $\gamma_{E_1E_1}$ and the slope of generalized polarizabilities $P^{(M_1, M_1)1} - P^{(L_1, L_1)1}$, measured in, respectively, the real and the virtual Compton scattering. We verify these sum rules in different variants of chiral perturbation theory, discuss their empirical verification for the proton, and prospect their use in studies of the nucleon spin structure.

Contents

I. Introduction	2
II. Sum rule derivation	3
A. Forward double virtual Compton scattering	3
B. Low-energy expansions	4
C. VVCS sum rules	6
1. Spin-independent amplitude T_1	6
2. Spin-independent amplitude T_2	7
3. Spin-dependent amplitude S_1	8
4. Spin-dependent amplitude S_2	9
III. Verification in heavy-baryon chiral perturbation theory	10
IV. Verification in covariant χPT	12
V. Empirical verification	14
VI. Predictions for the VCS response function P_{TT} at low Q^2	16
VII. Summary and Conclusion	19
Acknowledgments	19
References	20

I. INTRODUCTION

The low-energy nucleon structure is presently at the forefront of many precision studies of the Standard Model and beyond. Given the complexity of low-energy QCD, a popular method of calculating the nucleon-structure effects is the data-driven approach based on model-independent relations, such as sum rules. Perhaps the best known sum rule for the electromagnetic structure of the nucleon is the Gerasimov-Drell-Hearn (GDH) sum rule [1–3], relating the anomalous magnetic moment of the nucleon to a weighted integral over the polarized photo-absorption cross section. An even older sum rule is the one of Baldin [4], which gives the sum of the electric α_E and magnetic β_M dipole polarizabilities in terms the total cross section $\sigma(\nu)$ as follows:

$$\alpha_E + \beta_M = \frac{1}{2\pi^2} \int_{\nu_0}^{\infty} \frac{d\nu}{\nu^2} \sigma(\nu), \quad (1)$$

where ν is the photon energy in the laboratory frame, and ν_0 is the inelastic threshold. This sum rule has proven to be very useful for an accurate extraction of the nucleon polarizabilities, see Refs. [5–8] for reviews.

The Baldin sum rule, derived from general considerations of the forward Compton scattering amplitude, is easily generalized to the case of virtual photons, i.e., the forward double-virtual Compton scattering (VVCS). The sum of the two polarizabilities becomes dependent on the photon virtuality Q^2 , and is connected with the unpolarized nucleon structure function F_1 , measured in electron-nucleon scattering, via

$$\alpha_E(Q^2) + \beta_M(Q^2) = \frac{8\alpha_{\text{em}}M}{Q^4} \int_0^{x_0} dx x F_1(x, Q^2), \quad (2)$$

where M is the nucleon mass, α_{em} is the fine structure constant, and $x = Q^2/2M\nu$ is the Bjorken scaling variable with x_0 corresponding to the inelastic threshold. Other forward sum rules involving the spin dependent nucleon structure functions allow for such a generalization [9, 10], too. In this way, one can characterize the spin-dependent VVCS process through Q^2 -dependent transverse (γ_0) or transverse-longitudinal (δ_{LT}) spin polarizabilities of the nucleon [5, 11, 12]. These polarizabilities are thus related with the nucleon spin-dependent structure functions, and have been the subject of dedicated experimental activities at the Jefferson Lab, see [13, 14] for reviews.

The nucleon's response to external electromagnetic fields can also be probed through the virtual Compton scattering (VCS) process, in which the initial photon has finite virtuality Q^2 whereas the final one is real. The linear response of a nucleon in the low-energy VCS process can be expressed through generalized polarizabilities (GPs) [15], see Ref. [16] for a detailed review. The GPs, which encode the spatial distribution of the polarization densities in a nucleon [17], have been the subject of several dedicated experiments at MAMI [18–22], MIT-Bates [23, 24], and JLab [25, 26].

As the VCS process is a non-forward process and apparently asymmetric under photon crossing, it has precluded an immediate connection, via sum rules, of GPs with photoabsorption cross sections. Nonetheless, a new type of relation, presented recently in Ref. [27], allows to relate two of the spin-dependent GPs with quantities measured in RCS and VVCS. The new relations provide an extension of the GDH sum rule to finite virtuality, and as a result involve new quantities which are accessible in independent experiments.

In this work we provide a detailed derivation of the two new sum rules. We first discuss the forward double virtual Compton scattering (Section II A), its low-energy expansions (Section II B), and the derivation of forward sum rules for the four amplitudes characterizing the VVCS on the nucleon (Section II C). We then show how these sum rules are satisfied in heavy baryon chiral perturbation theory (Section III) as well as in its covariant counterpart — baryon chiral perturbation theory (Section IV). We discuss the phenomenological status of these sum rules and further experimental opportunities in Section V. In particular, by using the sum rules, we will obtain an empirical prediction for the slope of one of the VCS response functions, denoted by P_{TT} , and will compare it with the dispersive evaluations and with the predictions of baryon chiral perturbation theory calculations (Section VI). Finally, we will present our conclusions in Section VII.

II. SUM RULE DERIVATION

A. Forward double virtual Compton scattering

Our starting point is the double-virtual Compton on a nucleon

$$\gamma^*(q, \lambda) + N(p, s) \rightarrow \gamma^*(q', \lambda') + N(p', s'), \quad (3)$$

where λ, λ' denote the photon helicities, and s, s' are the nucleon helicities. This process is described by 18 helicity amplitudes introduced as:

$$T_{\lambda'\lambda s} \equiv e^2 \varepsilon_\mu(q, \lambda) \varepsilon_\nu^*(q', \lambda') \bar{u}(p', s') M^{\mu\nu} u(p, s), \quad (4)$$

where e is the proton electric charge, and ε_μ (ε_ν^*) stands for the initial (final) nuclear polarization vector. The double virtual Compton tensor $M^{\mu\nu}$ can be Lorentz-decomposed as (in the notation of Ref. [28]):

$$M^{\mu\nu} = \sum_{i \in J} B_i(q^2, q'^2, q \cdot q', q \cdot P) T_i^{\mu\nu}, \quad (5)$$

$$J = \{1, \dots, 21\} \setminus \{5, 15, 16\},$$

where $P = \frac{1}{2}(p + p')$. The 18 independent tensors $T_i^{\mu\nu}$ can be constructed to be gauge invariant, and free of kinematical singularities as shown by Tarrach [29]. The invariant amplitudes B_i have definite transformation properties with respect to the photon crossing, as well as charge conjugation combined with nucleon crossing [28]. The latter reference also contains the low-energy expansions of B_i 's up to $\mathcal{O}(k^3)$ ($k = \{q, q'\}$), which will be useful in the following.

To derive the sum rules one considers the *forward* double VCS process (VVCS), which is a special case of the process (3), with $q' = q$ and $p' = p$. The VVCS process is described by the four invariant amplitudes, denoted by T_1, T_2, S_1, S_2 , which are functions of $Q^2 \equiv -q^2$ and $\nu \equiv p \cdot q/M$. Its covariant tensor structure can be written as:

$$\alpha_{\text{em}} M^{\mu\nu}(\nu, Q^2) = - \left\{ \left(-g^{\mu\nu} + \frac{q^\mu q^\nu}{q^2} \right) T_1(\nu, Q^2) + \frac{1}{M^2} \left(p^\mu - \frac{p \cdot q}{q^2} q^\mu \right) \left(p^\nu - \frac{p \cdot q}{q^2} q^\nu \right) T_2(\nu, Q^2) \right. \\ \left. + \frac{i}{M} \epsilon^{\nu\mu\alpha\beta} q_\alpha s_\beta S_1(\nu, Q^2) + \frac{i}{M^3} \epsilon^{\nu\mu\alpha\beta} q_\alpha (p \cdot q s_\beta - s \cdot q p_\beta) S_2(\nu, Q^2) \right\}, \quad (6)$$

where the fine-structure constant $\alpha_{\text{em}} \equiv e^2/4\pi \simeq 1/137$ is conventionally introduced in defining the forward amplitudes T_1, T_2, S_1 , and S_2 . Furthermore, $\epsilon_{0123} = +1$, and s^α is the nucleon covariant spin vector satisfying $s \cdot p = 0$, $s^2 = -1$. The optical theorem relates the imaginary parts of the four amplitudes appearing in Eq. (6) to the four structure functions of inclusive electron-nucleon scattering as:

$$\text{Im } T_1(\nu, Q^2) = \frac{e^2}{4M} F_1(x, Q^2) \quad , \quad \text{Im } T_2(\nu, Q^2) = \frac{e^2}{4\nu} F_2(x, Q^2), \\ \text{Im } S_1(\nu, Q^2) = \frac{e^2}{4\nu} g_1(x, Q^2) \quad , \quad \text{Im } S_2(\nu, Q^2) = \frac{e^2 M}{4\nu^2} g_2(x, Q^2), \quad (7)$$

where $x \equiv Q^2/2M\nu$, and where F_1, F_2, g_1, g_2 are the conventionally defined structure functions which parametrize inclusive electron-nucleon scattering. The imaginary parts of the forward scattering amplitudes, Eqs. (7), get contributions from both elastic scattering at $\nu = \nu_B \equiv Q^2/(2M)$ or equivalently $x = 1$, as well as from inelastic processes above the pion threshold, corresponding with $\nu > \nu_0 \equiv m_\pi + (Q^2 + m_\pi^2)/(2M)$ or equivalently $x < x_0 \equiv Q^2/(2M\nu_0)$. The elastic contributions are obtained as pole parts of the direct and crossed nucleon Born diagrams. The latter are conventionally separated off the Compton scattering tensor in order to define structure-dependent constants, such as polarizabilities. The Born terms are defined by using the electromagnetic vertex for the transition $\gamma^*(q) + N(p) \rightarrow N(p+q)$ as given by

$$\Gamma^\mu = F_D(Q^2) \gamma^\mu + F_P(Q^2) i\sigma^{\mu\nu} \frac{q_\nu}{2M}, \quad (8)$$

with F_D and F_P the Dirac and Pauli form factors of nucleon N , normalized to $F_D(0) = e_N$ and $F_P(0) = \kappa_N$, where e_N is the charge in units of e , and where κ_N is the anomalous magnetic moment in units of $e/2M$;

$\sigma^{\mu\nu} = (i/2)[\gamma^\mu, \gamma^\nu]$. This choice of the electromagnetic vertex ensures that the Born contributions are gauge invariant and leads to the following contributions:

$$\begin{aligned} T_1^{\text{Born}} &= -\frac{\alpha_{\text{em}}}{M} \left(F_D^2 + \frac{\nu_B^2}{\nu^2 - \nu_B^2 + i\varepsilon} G_M^2 \right), & T_2^{\text{Born}} &= -\frac{\alpha_{\text{em}}}{M} \frac{Q^2}{\nu^2 - \nu_B^2 + i\varepsilon} (F_D^2 + \tau F_P^2), \\ S_1^{\text{Born}} &= -\frac{\alpha_{\text{em}}}{2M} \left(F_P^2 + \frac{Q^2}{\nu^2 - \nu_B^2 + i\varepsilon} F_D G_M \right), & S_2^{\text{Born}} &= \frac{\alpha_{\text{em}}}{2} \frac{\nu}{\nu^2 - \nu_B^2 + i\varepsilon} F_P G_M, \end{aligned} \quad (9)$$

with $G_M(Q^2) = F_D(Q^2) + F_P(Q^2)$, and $\tau \equiv Q^2/4M^2$. The Born contributions of Eq. (9) can be split into non-pole and pole contributions in a dispersion relation framework. The pole contributions (also called elastic contributions) can be immediately read off Eqs. (9). Their real parts are given by

$$\begin{aligned} \text{Re } T_1^{\text{pole}} &= -\frac{\alpha_{\text{em}}}{M} \frac{\nu_B^2}{\nu^2 - \nu_B^2} G_M^2, & \text{Re } T_2^{\text{pole}} &= -\frac{\alpha_{\text{em}}}{M} \frac{Q^2}{\nu^2 - \nu_B^2} (F_D^2 + \tau F_P^2), \\ \text{Re } S_1^{\text{pole}} &= -\frac{\alpha_{\text{em}}}{2M} \frac{Q^2}{\nu^2 - \nu_B^2} F_D G_M, & \text{Re } (\nu S_2^{\text{pole}}) &= \frac{\alpha_{\text{em}}}{2} \frac{\nu_B^2}{\nu^2 - \nu_B^2} F_P G_M, \end{aligned} \quad (10)$$

B. Low-energy expansions

Following Ref. [28], in order to obtain a low-energy expansion (LEX) in $k = \{\nu, Q\}$ for the forward VCS amplitudes T_1, T_2, S_1 , and S_2 , we express them in terms of the B_i of Eq. (5):

$$T_1(\nu, Q^2) = \alpha_{\text{em}} \{ Q^2 B_1 - 4M^2 \nu^2 B_2 + Q^4 B_3 - 4M\nu Q^2 B_4 \}, \quad (11a)$$

$$T_2(\nu, Q^2) = \alpha_{\text{em}} 4M^2 Q^2 \{ -B_2 - Q^2 B_{19} \}, \quad (11b)$$

$$S_1(\nu, Q^2) = \alpha_{\text{em}} M \{ -4M\nu B_7 + Q^2 [B_8 + M(4B_{10} + 2B_{21}) + 4B_{18}] \}, \quad (11c)$$

$$S_2(\nu, Q^2) = \alpha_{\text{em}} M^2 \left\{ -\frac{Q^2}{2} B_6 - 2B_{17} + M\nu(4B_{10} + 2B_{21}) - Q^2 B_{12} \right\}, \quad (11d)$$

where the B_i also depend on ν and Q^2 for forward kinematics. We can next use the expansions in $k = \{\nu, Q\}$ established in [28]:

$$B_i = b_{i,0} + \mathcal{O}(k^2), \quad (i = 1, 2, 3, 8, 10, 18, 19, 21), \quad (12)$$

$$B_i = 2M\nu [b_{i,1} + \mathcal{O}(k^2)], \quad (i = 4, 6, 7, 12, 17), \quad (13)$$

where $b_{i,0}$ and $b_{i,1}$ are low-energy constants. As we are only interested in the lowest-order terms in $k = \{\nu, Q\}$, we obtain the following LEXs for Eqs. (11a)–(11d):

$$T_1(\nu, Q^2) = \alpha_{\text{em}} \{ Q^2 b_{1,0} - 4M^2 \nu^2 b_{2,0} + \mathcal{O}(k^4) \}, \quad (14a)$$

$$T_2(\nu, Q^2) = -\alpha_{\text{em}} \{ 4M^2 Q^2 b_{2,0} + \mathcal{O}(k^4) \}, \quad (14b)$$

$$S_1(\nu, Q^2) = \alpha_{\text{em}} M \{ -8M^2 \nu^2 b_{7,1} + Q^2 [b_{8,0} + M(4b_{10,0} + 2b_{21,0}) + 4b_{18,0}] + \mathcal{O}(k^4) \}, \quad (14c)$$

$$S_2(\nu, Q^2) = \alpha_{\text{em}} M^3 \nu \{ -4b_{17,1} + 4b_{10,0} + 2b_{21,0} + \mathcal{O}(k^2) \}. \quad (14d)$$

Of the eight coefficients appearing in Eqs. (14a)–(14d), six can be related to the scalar and spin dipole polarizabilities as measured in real Compton scattering (RCS). As polarizabilities are conventionally defined by separating off the Born parts of the amplitudes, one splits the amplitudes into Born and non-Born parts as $T_1 = T_1^{\text{Born}} + T_1^{\text{nB}}$, and analogously for the other three amplitudes. The Born parts are given by Eqs. (9).

The non-Born (nB) parts of six of the low-energy constants are then expressed in terms of polarizabilities:

$$b_{1,0}^{\text{nB}} = \frac{1}{\alpha_{\text{em}}} \beta_M, \quad (15\text{a})$$

$$b_{2,0}^{\text{nB}} = -\frac{1}{\alpha_{\text{em}}} \frac{1}{4M^2} (\alpha_E + \beta_M), \quad (15\text{b})$$

$$b_{7,1}^{\text{nB}} = -\frac{1}{\alpha_{\text{em}}} \frac{1}{8M^2} \gamma_0, \quad (15\text{c})$$

$$b_{10,0}^{\text{nB}} = \frac{1}{\alpha_{\text{em}}} \frac{1}{4M} (\gamma_{M1E2} + \gamma_{E1M2}), \quad (15\text{d})$$

$$b_{17,1}^{\text{nB}} = \frac{1}{\alpha_{\text{em}}} \frac{1}{4M} (\gamma_{M1E2} - \gamma_{M1M1}), \quad (15\text{e})$$

$$b_{18,0}^{\text{nB}} = -\frac{1}{\alpha_{\text{em}}} \frac{1}{2} \gamma_{M1E2}, \quad (15\text{f})$$

where α_E (β_M) are the electric (magnetic) dipole polarizabilities respectively, and γ_{M1E2} , γ_{E1M2} , γ_{M1M1} , γ_{E1E1} are the lowest-order spin polarizabilities of the nucleon, which are related to the forward spin polarizability γ_0 as:

$$\gamma_0 = -(\gamma_{M1E2} + \gamma_{E1M2} + \gamma_{M1M1} + \gamma_{E1E1}). \quad (16)$$

We notice from Eqs. (14a)–(14b) and Eqs. (15a)–(15b) that the electric and magnetic dipole polarizabilities measured in RCS fully determine the terms of order ν^2 and Q^2 in the LEXs of both VVCS amplitudes T_1 and T_2 . In order to fully specify the LEXs for the spin-dependent forward VCS amplitudes S_1 , and S_2 , we need in addition the coefficients $b_{8,0}$ and $b_{21,0}$. We next show how they can be related to two of the generalized polarizabilities (GPs), determined from the (non-forward) VCS process

$$\gamma^*(q) + N(p) \rightarrow \gamma(q') + N(p'), \quad (17)$$

where the outgoing photon is real and carries a low momentum, i.e. $q'^2 = 0$ and $q' \rightarrow 0$.

The VCS experiments at low outgoing photon energies can also be analyzed in terms of LEXs, as proposed in Ref. [15]. The VCS tensor describing the process (17) has been split in Ref. [15] into a Born part, which is defined as the nucleon intermediate state contribution using the $\gamma^* \gamma N$ vertex of Eq. (8), and a non-Born part. The latter describes the response of the nucleon to the quasi-static electromagnetic field, due to the nucleon's internal structure. For the lowest-order nucleon-structure terms, one considers the response linear in the energy of the produced real photon. The VCS tensor describing the process (17) can generally be parametrized in terms of 12 independent amplitudes. In Ref. [28], a gauge-invariant tensor basis was constructed such that the non-Born invariant amplitudes are free of kinematical singularities and constraints:

$$M^{\mu\nu} = \sum_{i=1}^{12} f_i(q^2, q \cdot q', q \cdot P) \rho_i^{\mu\nu}, \quad (18)$$

where the explicit expression for the tensors $\rho_i^{\mu\nu}$ can be found in Ref. [28]. Furthermore in the limit $q'^2 = 0$, the 12 invariant amplitudes f_i are related with the invariants B_i of Eq. (5), describing the doubly-virtual Compton scattering process:

$$\begin{aligned} f_1 &= B_1, & f_2 &= B_2, & f_3 &= B_4, \\ f_4 &= B_7, & f_5 &= B_8 - B_9, & f_6 &= B_{10}, \\ f_7 &= B_{11}, & f_8 &= B_{12} + B_{13}, & f_9 &= B_{14}, \\ f_{10} &= B_{17}, & f_{11} &= B_{18}, & f_{12} &= B_{20} + B_{21}, \end{aligned} \quad (19)$$

where the limit $q'^2 = 0$ is taken in the argument of the B_i .

The behavior of the non-Born VCS tensor at low energy ($q' \rightarrow 0$) but at arbitrary three-momentum \bar{q} of the virtual photon, which is conveniently defined in the c.m. system of the $\gamma^* N$ system, can be parametrized by six independent GPs [15, 28]. The GPs can be accessed in experiment through the $eN \rightarrow eN\gamma$ process;

see the reviews [5, 16] for more details. At lowest order in the outgoing photon energy, there are two spin-independent GPs, denoted by $P^{(L1,L1)0}$, $P^{(M1,M1)0}$, and four spin GPs, denoted by $P^{(L1,M2)1}$, $P^{(M1,L2)1}$, $P^{(L1,L1)1}$, and $P^{(M1,M1)1}$, which are all functions of Q^2 .¹ In this notation, L stands for the longitudinal (or electric) and M for the magnetic nature of the transition respectively. At $Q^2 = 0$, four of the six GPs are related to the polarizabilities from RCS as

$$\begin{aligned}\alpha_E &= -\alpha_{\text{em}} \frac{\sqrt{3}}{\sqrt{2}} P^{(L1,L1)0}(0), & \beta_M &= -\alpha_{\text{em}} \frac{\sqrt{3}}{2\sqrt{2}} P^{(M1,M1)0}(0), \\ \gamma_{E1M2} &= -\alpha_{\text{em}} \frac{3}{\sqrt{2}} P^{(L1,M2)1}(0), & \gamma_{M1E2} &= -\alpha_{\text{em}} \frac{3\sqrt{3}}{2\sqrt{2}} P^{(M1,L2)1}(0),\end{aligned}\quad (20)$$

whereas the remaining two GPs vanish in the real photon limit, i.e. $P^{(L1,L1)1}(0) = 0$, and $P^{(M1,M1)1}(0) = 0$.

The GPs can be expressed through the non-Born (nB) parts of the invariant amplitudes f_i . Using the shorthand notation,

$$\bar{f}_i(Q^2) \equiv f_i^{\text{nB}}(q^2 = -Q^2, 0, 0), \quad (21)$$

together with Eq. (19), these expressions are [28]:

$$b_{8,0}^{\text{nB}} = \bar{f}_5(0) = -6MP^{(M1,M1)1}(0), \quad (22)$$

$$b_{21,0}^{\text{nB}} = \bar{f}_{12}(0) = \frac{3}{2} \left[P^{(M1,M1)1}(0) - P^{(L1,L1)1}(0) \right] + \frac{1}{\alpha_{\text{em}}} \frac{1}{2M} \gamma_{M1E2}. \quad (23)$$

In Eqs. (22, 23) we have introduced the notations for the slopes at $Q^2 = 0$ of two GPs as:

$$P^{(L1,L1)1}(0) \equiv \left. \frac{d}{dQ^2} P^{(L1,L1)1}(Q^2) \right|_{Q^2=0}, \quad (24)$$

$$P^{(M1,M1)1}(0) \equiv \left. \frac{d}{dQ^2} P^{(M1,M1)1}(Q^2) \right|_{Q^2=0}. \quad (25)$$

We note that the lowest-order polarizabilities as measured through RCS together with the slopes at $Q^2 = 0$ of the two lowest-order GPs which themselves vanish at $Q^2 = 0$, and thus require a measurement through the VCS process, specify all low-energy constants appearing in the VVCS amplitudes of Eqs. (14a-14d).

C. VVCS sum rules

Having established the LEXs of the forward double VCS amplitudes T_1, T_2, S_1 and S_2 , we are ready to use the analyticity in ν , for fixed spacelike photon virtuality, i.e. $Q^2 \geq 0$. We distinguish two cases depending on their symmetry under $s \leftrightarrow u$ crossing, which flips the sign of ν : the amplitudes T_1, T_2 and S_1 are even functions of ν whereas S_2 is odd. We will present the relations for the non-pole parts of the amplitudes, $T_1^{\text{np}}(\nu, Q^2) = T_1(\nu, Q^2) - T_1^{\text{pole}}(\nu, Q^2)$ etc., i.e., the well-known pole amplitudes given by Eq. (10) are subtracted from the full amplitudes.

1. Spin-independent amplitude T_1

The dispersion relation for T_1 requires one subtraction, which we take at $\nu = 0$, in order to ensure high-energy convergence :

$$\text{Re } T_1^{\text{np}}(\nu, Q^2) = \text{Re } T_1^{\text{np}}(0, Q^2) + \frac{\nu^2}{2\pi} \mathcal{P} \int_{\nu_0}^{\infty} d\nu' \frac{1}{\nu'(\nu'^2 - \nu^2)} \frac{e^2}{M} F_1(x', Q^2), \quad (26)$$

¹ Equivalently, they can be considered as functions of $\bar{q}^2 = Q^2(1 + \tau)$; this definition is used in Ref. [15].

with $x' \equiv Q^2/(2M\nu')$. Because the non-pole amplitudes are analytic functions of ν , they can be expanded in a Taylor series about $\nu = 0$ with a convergence radius determined by the lowest singularity, the threshold of pion production at $\nu = \nu_0$. Analogous to the low-energy expansion of RCS, the series in ν , at fixed value of Q^2 , for forward double VCS takes the following form [5]:

$$T_1^{\text{np}}(\nu, Q^2) = T_1^{\text{np}}(0, Q^2) + (\alpha_E(Q^2) + \beta_M(Q^2)) \nu^2 + \mathcal{O}(\nu^4), \quad (27)$$

The coefficients of the Taylor series of Eq. (27) follow by expanding the dispersion integrals as function of ν . This yields a generalization of Baldin's sum rule for the forward dipole polarizabilities [5]:

$$\alpha_E(Q^2) + \beta_M(Q^2) = \frac{e^2 M}{\pi Q^4} \int_0^{x_0} dx 2x F_1(x, Q^2), \quad (28)$$

where x_0 corresponds with the pion production threshold. We next discuss the subtraction function at $\nu = 0$, $T_1^{\text{np}}(0, Q^2)$, entering the dispersion relation of Eq. (26). Although in general the Q^2 behavior of this function is unknown, one can express its behavior at low Q^2 in terms of polarizabilities, see, e.g., Ref. [30]. We like to emphasize that polarizabilities are conventionally defined by separating the Compton amplitudes into Born and non-Born parts, with Born parts given by Eqs. (9). The non-Born part of T_1 can then be read off Eqs. (14a), (15a), (15b) as

$$T_1^{\text{nB}}(\nu, Q^2) = (\alpha_E + \beta_M) \nu^2 + \beta_M Q^2 + \mathcal{O}(k^4), \quad (29)$$

with $k = \{\nu, Q\}$. To obtain the low-energy expansion in k of the non-pole part T_1^{np} entering Eq. (26), we also need to account for the difference between the Born and pole parts, which can be easily read off Eq. (9) as

$$T_1^{\text{Born}}(\nu, Q^2) - T_1^{\text{pole}}(\nu, Q^2) = -\frac{\alpha_{\text{em}}}{M} F_D^2 = -\frac{\alpha_{\text{em}}}{M} e_N^2 + \frac{\alpha_{\text{em}}}{3M} e_N \langle r_1^2 \rangle Q^2 + \mathcal{O}(Q^4), \quad (30)$$

where $\langle r_1^2 \rangle$ is the squared Dirac radius of the nucleon. Combining Eqs. (29) and (30), one then obtains the low-energy expansion of T_1^{np} in both ν^2 and Q^2 as

$$T_1^{\text{np}}(\nu, Q^2) = -\frac{\alpha_{\text{em}}}{M} e_N^2 + (\alpha_E + \beta_M) \nu^2 + \left(\frac{\alpha_{\text{em}}}{3M} e_N \langle r_1^2 \rangle + \beta_M \right) Q^2 + \mathcal{O}(k^4). \quad (31)$$

Consequently, the subtraction function at $\nu = 0$, which enters the dispersion relations of Eq. (26), is given up to terms of order $\mathcal{O}(Q^4)$ by

$$T_1^{\text{np}}(0, Q^2) = -\frac{\alpha_{\text{em}}}{M} e_N^2 + \left(\frac{\alpha_{\text{em}}}{3M} e_N \langle r_1^2 \rangle + \beta_M \right) Q^2 + \mathcal{O}(Q^4). \quad (32)$$

2. Spin-independent amplitude T_2

For the amplitude T_2 , which is even in ν , one can write down an unsubtracted DR in ν :

$$\text{Re } T_2^{\text{np}}(\nu, Q^2) = \frac{1}{2\pi} \mathcal{P} \int_{\nu_0}^{\infty} d\nu' \frac{1}{\nu'^2 - \nu^2} e^2 F_2(x', Q^2). \quad (33)$$

The expansion of the amplitude T_2 at small $k = \{\nu, Q\}$ can be read off Eqs. (14a, 15b) as ²

$$T_2^{\text{np}}(\nu, Q^2) = (\alpha_E + \beta_M) Q^2 + \mathcal{O}(k^4). \quad (34)$$

By evaluating Eq. (33) at $\nu = 0$, taking its derivative with respect to Q^2 at $Q^2 = 0$, and using the relation

$$\left[\frac{1}{Q^2} F_2(x, Q^2) \right]_{Q^2=0} = \left[\frac{1}{Q^2} 2x F_1(x, Q^2) \right]_{Q^2=0} = \frac{1}{e^2 \pi} \sigma_T, \quad (35)$$

with σ_T the total (real) photon absorption cross section, one recovers the Baldin sum rule [4], i.e. Eq. (28) evaluated at $Q^2 = 0$, for $(\alpha_E + \beta_M)$.

² For the amplitude T_2 , there is no difference between the Born and pole contributions, as seen from Eq. (9).

3. Spin-dependent amplitude S_1

We next discuss the DR for the spin-dependent amplitude S_1 . The amplitude S_1 is even in ν , and the unsubtracted DR for its non-pole part reads

$$\text{Re } S_1^{\text{np}}(\nu, Q^2) = \frac{1}{2\pi} \mathcal{P} \int_{\nu_0}^{\infty} d\nu' \frac{\nu'}{\nu'^2 - \nu^2} \frac{e^2}{\nu'} g_1(x', Q^2). \quad (36)$$

The low-energy expansion in ν , at fixed value of Q^2 , for S_1^{np} takes the form [5]

$$S_1^{\text{np}}(\nu, Q^2) = \frac{2\alpha_{\text{em}}}{M} I_1(Q^2) + \left[\frac{2\alpha_{\text{em}}}{M Q^2} \left(I_{TT}(Q^2) - I_1(Q^2) \right) + M \delta_{LT}(Q^2) \right] \nu^2 + \mathcal{O}(\nu^4), \quad (37)$$

where the leading term of $\mathcal{O}(\nu^0)$ follows from Eq. (36) as

$$I_1(Q^2) = \frac{2M^2}{Q^2} \int_0^{x_0} dx g_1(x, Q^2). \quad (38)$$

Using Eqs. (9) and (14c) one obtains the low-energy theorem result : $S_1^{\text{np}}(0, 0) = -\alpha_{\text{em}} \kappa_N^2 / (2M)$, which yields the GDH sum rule for real photons [2, 3], $I_1(0) = -\kappa_N^2 / 4$. The ν^2 -dependent term in the expansion of Eq. (37) involves, besides I_1 , also the moment I_{TT} of the helicity difference cross sections and a longitudinal-transverse polarizability δ_{LT} , which are expressed through moments of spin structure functions as [5]

$$I_{TT}(Q^2) = \frac{2M^2}{Q^2} \int_0^{x_0} dx \left\{ g_1(x, Q^2) - \frac{4M^2}{Q^2} x^2 g_2(x, Q^2) \right\}, \quad (39)$$

$$\delta_{LT}(Q^2) = \frac{4e^2 M^2}{\pi Q^6} \int_0^{x_0} dx x^2 \{ g_1(x, Q^2) + g_2(x, Q^2) \}. \quad (40)$$

At $Q^2 = 0$, the ν^2 term in the low-energy expansion of S_1^{np} can be read off Eqs. (14c) and (15c), yielding ³

$$S_1^{\text{np}}(\nu, 0) = \frac{2\alpha_{\text{em}}}{M} \left(-\frac{\kappa_N^2}{4} \right) + M \gamma_0 \nu^2 + \mathcal{O}(\nu^4), \quad (41)$$

where γ_0 is the forward spin polarizability as accessed in RCS, which can be obtained as the $Q^2 \rightarrow 0$ limit of the integral obtained in Ref. [5]:

$$\gamma_0(Q^2) = \frac{4M^2 e^2}{\pi Q^6} \int_0^{x_0} dx x^2 \left\{ g_1(x, Q^2) - \frac{4M^2}{Q^2} x^2 g_2(x, Q^2) \right\}. \quad (42)$$

We can derive a new sum rule by performing a Taylor series in Q^2 at $\nu = 0$ for S_1^{np} . By expanding $I_1(Q^2)$ in Eq. (37), we obtain

$$S_1^{\text{np}}(0, Q^2) = \frac{2\alpha_{\text{em}}}{M} \left\{ -\frac{\kappa_N^2}{4} + Q^2 I_1'(0) + \mathcal{O}(Q^4) \right\}, \quad (43)$$

where $I_1'(0) \equiv \left. \frac{d}{dQ^2} I_1(Q^2) \right|_{Q^2=0}$ is the Q^2 slope at $Q^2 = 0$ of the first moment of the structure function g_1 .

Using the low-energy expansion of Eq. (14c), we can identify the Q^2 -dependent term of the non-Born part S_1^{nb} at $\nu = 0$ as

$$\begin{aligned} S_1^{\text{nb}}(0, Q^2) &= \alpha_{\text{em}} M Q^2 \{ 4M b_{10,0}^{\text{nb}} + 4 b_{18,0}^{\text{nb}} + b_{8,0}^{\text{nb}} + 2M b_{21,0}^{\text{nb}} \} + \mathcal{O}(Q^4), \\ &= \alpha_{\text{em}} M Q^2 \left\{ \frac{1}{\alpha_{\text{em}}} \gamma_{E1M2} - 3M \left[P'^{(M1,M1)1}(0) + P'^{(L1,L1)1}(0) \right] \right\} + \mathcal{O}(Q^4), \end{aligned} \quad (44)$$

³ Note that this implies the relation [5]: $I'_{TT}(0) - I'_1(0) = \frac{M^2}{2\alpha_{\text{em}}} (\gamma_0 - \delta_{LT})$, with $I'_i(0) \equiv \left. \frac{d}{dQ^2} I_i(Q^2) \right|_{Q^2=0}$, and $\delta_{LT} \equiv \delta_{LT}(0)$.

where in the last line we have used Eqs. (15d), (15f), (22), (23) for the corresponding low-energy coefficients. To relate $I_1'(0)$ with the expression in Eq. (44), we need to account for the difference between Born and pole parts, which can be read off Eq. (9) as

$$S_1^{\text{Born}}(\nu, Q^2) - S_1^{\text{pole}}(\nu, Q^2) = -\frac{\alpha_{\text{em}}}{2M} F_P^2 = \frac{2\alpha_{\text{em}}}{M} \left\{ -\frac{\kappa_N^2}{4} + \frac{\kappa_N^2}{12} \langle r_2^2 \rangle Q^2 + \mathcal{O}(Q^4) \right\}, \quad (45)$$

where $\langle r_2^2 \rangle$ is the nucleon mean squared Pauli radius. Combining Eqs. (43), (44), and (45) then allows us to derive a new sum rule relating the slope at $Q^2 = 0$ of the GDH sum rule to the Pauli radius and polarizabilities as measured in RCS and VCS:

$$I_1'(0) = \frac{\kappa_N^2}{12} \langle r_2^2 \rangle + \frac{M^2}{2} \left\{ \frac{1}{\alpha_{\text{em}}} \gamma_{E1M2} - 3M \left[P'^{(M1, M1)1}(0) + P'^{(L1, L1)1}(0) \right] \right\}. \quad (46)$$

We like to emphasize that all quantities entering Eq. (46) are observable quantities: the *lhs* is obtained from the first moment of the spin structure function g_1 [13, 14], whereas the *rhs* involves the Pauli radius as well as spin polarizabilities measured through the RCS and VCS processes. Therefore the sum rule of Eq. (46) provides us with a model-independent and predictive relation. In the next sections, we will test this new GDH sum rule for finite photon virtuality using heavy-baryon as well as covariant baryon chiral perturbation theory. We will also provide a phenomenological evaluation based on available data.

4. Spin-dependent amplitude S_2

Finally, for the second spin-dependent forward double VCS amplitude S_2 , which is odd in ν , an unsubtracted DR takes the form

$$\text{Re } S_2(\nu, Q^2) = \text{Re } S_2^{\text{pole}}(\nu, Q^2) + \frac{\nu}{2\pi} \mathcal{P} \int_{\nu_0}^{\infty} d\nu' \frac{1}{\nu'^2 - \nu^2} \frac{e^2 M}{\nu'^2} g_2(x', Q^2). \quad (47)$$

If we further assume that the amplitude S_2 converges faster than $1/\nu$ for $\nu \rightarrow \infty$, we may write an unsubtracted dispersion relation for the amplitude νS_2 , which is even in ν ,

$$\text{Re } [\nu S_2(\nu, Q^2)] = \text{Re } [\nu S_2(\nu, Q^2)]^{\text{pole}} + \frac{1}{2\pi} \mathcal{P} \int_{\nu_0}^{\infty} d\nu' \frac{1}{\nu'^2 - \nu^2} e^2 M g_2(x', Q^2). \quad (48)$$

If we now multiply Eq. (47) by ν and subtract it from Eq. (48), we obtain the Burkhardt-Cottingham (BC) ‘‘superconvergence sum rule’’ [31], valid for *any* value of Q^2 :

$$\int_0^1 g_2(x, Q^2) dx = 0, \quad (49)$$

provided that the integral converges for $x \rightarrow 0$. Notice that the upper integration limit in the integral of Eq. (49) extends to 1, and thus includes the elastic contribution. By separating the elastic and inelastic parts in the integral of Eq. (49), the BC sum rule can be cast into the equivalent form

$$I_2(Q^2) \equiv \frac{2M^2}{Q^2} \int_0^{x_0} g_2(x, Q^2) dx = \frac{1}{4} F_P(Q^2) G_M(Q^2). \quad (50)$$

The BC sum rule was shown to be satisfied in quantum electrodynamics by an explicit calculation at lowest order in the coupling constant α_{em} [32]. In perturbative QCD, the BC sum rule was verified for a quark target to first order in α_s [33]. Furthermore, in the non-perturbative domain of low Q^2 , the BC sum rule was also verified within heavy-baryon chiral perturbation theory [34, 35].

The LEX of $(\nu S_2)^{\text{np}}$ can be expressed as [5]

$$[\nu S_2(\nu, Q^2)]^{\text{np}} = 2\alpha_{\text{em}} I_2(Q^2) + \frac{2\alpha_{\text{em}}}{Q^2} I_2^{(3)}(Q^2) \nu^2 + \mathcal{O}(\nu^4), \quad (51)$$

where the observable $I_2^{(3)}(Q^2)$ is defined through the third moment of the spin structure function g_2 as

$$I_2^{(3)}(Q^2) \equiv \frac{8M^4}{Q^4} \int_0^{x_0} dx x^2 g_2(x, Q^2), \quad (52)$$

$$= I_1(Q^2) - I_{TT}(Q^2), \quad (53)$$

and where the last line has been obtained by using Eqs. (38) and (39). Note that the slope at $Q^2 = 0$ of $I_2^{(3)}(Q^2)$ follows from footnote 3 as

$$I_2^{(3)'}(0) = \frac{M^2}{2\alpha_{em}} (\delta_{LT} - \gamma_0). \quad (54)$$

Using the low-energy expansion of Eq. (14d), we can identify the ν^2 dependent term of the non-Born part of νS_2^{nB} as

$$\nu S_2^{\text{nB}}(\nu, Q^2) = \alpha_{em} M^3 \nu^2 \{4 b_{10,0}^{\text{nB}} - 4 b_{17,1}^{\text{nB}} + 2 b_{21,0}^{\text{nB}}\} + \mathcal{O}(\nu^4, \nu^2 Q^2), \quad (55)$$

To relate Eqs. (51) and (55), we need to account for the difference between Born and pole parts, which can be read off Eq. (9) as

$$\nu S_2^{\text{Born}}(\nu, Q^2) - [\nu S_2(\nu, Q^2)]^{\text{pole}} = \frac{\alpha_{em}}{2} F_P(Q^2) G_M(Q^2), \quad (56)$$

and precisely accounts for the leading term of $\mathcal{O}(\nu^0)$ in Eq. (51), as given by the BC sum rule, Eq. (50). The terms of $\mathcal{O}(\nu^2)$ in Eqs. (51) and (55) can then be identified to yield the new sum rule:

$$I_2^{(3)'}(0) = M^3 \{2 b_{10,0}^{\text{nB}} - 2 b_{17,1}^{\text{nB}} + b_{21,0}^{\text{nB}}\}. \quad (57)$$

On the *rhs* of Eq. (57), the low-energy quantities $b_{10,0}^{\text{nB}}$, $b_{17,1}^{\text{nB}}$, and $b_{21,0}^{\text{nB}}$ are related to polarizabilities as measured in RCS and VCS through Eqs. (15d), (15e), and (23). In this way we obtain the following sum rule:

$$I_2^{(3)'}(0) = \frac{M^2}{2} \left\{ -\frac{1}{\alpha_{em}} [\gamma_0 + \gamma_{E_1 E_1}] + 3M \left[P'^{(M_1, M_1)1}(0) - P'^{(L_1, L_1)1}(0) \right] \right\}. \quad (58)$$

Using Eq. (54), the sum rule of Eq. (58) can be expressed equivalently as

$$\delta_{LT} = -\gamma_{E_1 E_1} + 3M\alpha_{em} \left[P'^{(M_1, M_1)1}(0) - P'^{(L_1, L_1)1}(0) \right]. \quad (59)$$

Note that similar to its counterpart of Eq. (46), all quantities which enter Eq. (59) are observables. Therefore the new sum rule of Eq. (59) provides us with a second model-independent and predictive relation among low-energy spin structure constants of the nucleon.

III. VERIFICATION IN HEAVY-BARYON CHIRAL PERTURBATION THEORY

In this section we verify the new GDH sum rule of Eq. (46) for finite photon virtuality as well as the sum rule of Eq. (59) for δ_{LT} within the context of heavy-baryon chiral perturbation theory (HB χ PT). For the purpose of this verification, we will express the two sum rules of Eqs. (46) and (59) equivalently as relations for the GPs as

$$P'^{(M_1, M_1)1}(0) = \frac{1}{6M} \left\{ \frac{2}{M^2} \left(\frac{\kappa_N^2}{12} \langle r_2^2 \rangle - I_1'(0) \right) + \frac{1}{\alpha_{em}} (\gamma_{E_1 M_2} + \gamma_{E_1 E_1} + \delta_{LT}) \right\}, \quad (60)$$

$$P'^{(L_1, L_1)1}(0) = \frac{1}{6M} \left\{ \frac{2}{M^2} \left(\frac{\kappa_N^2}{12} \langle r_2^2 \rangle - I_1'(0) \right) + \frac{1}{\alpha_{em}} (\gamma_{E_1 M_2} - \gamma_{E_1 E_1} - \delta_{LT}) \right\}. \quad (61)$$

In HB χ PT, the leading order (LO) contribution in the chiral expansion of both of these sum rules corresponds with terms which are proportional to $1/m_\pi^2$, with m_π the pion mass. The next-to-leading order (NLO)

contribution corresponds with terms proportional to $1/(m_\pi M)$. All terms which are necessary to verify this sum rule have been calculated already up to NLO in the literature.

The evaluation of Eqs. (60), (61) involves the first moment $I_1(Q^2)$ of the g_1 structure function, which was evaluated in HB χ PT up to NLO in the chiral expansion as [10, 36]

$$I_1'(0) = \frac{g_A^2}{(4\pi f_\pi)^2} \frac{M}{m_\pi} \frac{\pi}{48} [1 + 3\kappa_V + (2 + 6\kappa_S)\tau_3], \quad (62)$$

where $f_\pi = 92.4$ MeV is the pion decay constant, $g_A = 1.27$ is the nucleon axial coupling constant, τ_3 is the third Pauli isospin matrix, and $\kappa_V = 3.70$ ($\kappa_S = -0.12$) denotes the nucleon isovector (isoscalar) anomalous magnetic moment.

Furthermore, the HB χ PT calculation of δ_{LT} , which appears in both Eqs. (60) and (61), was performed in Ref. [34] up to NLO in the chiral expansion:

$$\frac{1}{\alpha_{\text{em}}} \delta_{LT} = \frac{g_A^2}{(4\pi f_\pi)^2} \frac{1}{m_\pi^2} \frac{1}{3} \left\{ 1 + \frac{\pi}{8} \frac{m_\pi}{M} [-3 + \kappa_V + (-6 + 4\kappa_S)\tau_3] \right\}. \quad (63)$$

The first term on the *rhs* of Eqs. (60)–(61) involves the Pauli radius. To the order needed, its expression in HB χ PT is given by [37]

$$\frac{\kappa_N^2}{12} \langle r_2^2 \rangle = -\frac{\kappa_N}{2} F_P'(0) = \frac{g_A^2}{(4\pi f_\pi)^2} \frac{M}{m_\pi} \frac{\pi}{24} [\kappa_V + \kappa_S\tau_3]. \quad (64)$$

The nucleon spin polarizabilities $\gamma_{E1,M2}$ and $\gamma_{E1,E1}$, obtained from RCS, which appear on the *rhs* of Eqs. (60)–(61), are given up to NLO in the chiral expansion, i.e. $\mathcal{O}(p^4)$, as [38]

$$\frac{1}{\alpha_{\text{em}}} \gamma_{E1M2} = \frac{g_A^2}{(4\pi f_\pi)^2} \frac{1}{m_\pi^2} \frac{1}{6} \left\{ 1 - \frac{\pi}{4} \frac{m_\pi}{M} [6 + \tau_3] \right\}, \quad (65)$$

$$\frac{1}{\alpha_{\text{em}}} \gamma_{E1E1} = \frac{g_A^2}{(4\pi f_\pi)^2} \frac{1}{m_\pi^2} \frac{1}{6} \left\{ -5 + \frac{\pi}{4} \frac{m_\pi}{M} [22 + 11\tau_3] \right\}. \quad (66)$$

In this way, we obtain for the *rhs* of Eqs. (60)–(61)

$$\frac{1}{6M} \left\{ \frac{2}{M^2} \left(\frac{\kappa_N^2}{12} \langle r_2^2 \rangle - I_1'(0) \right) + \frac{1}{\alpha_{\text{em}}} (\gamma_{E1M2} + \gamma_{E1E1} + \delta_{LT}) \right\} = \frac{g_A^2}{(4\pi f_\pi)^2} \frac{1}{m_\pi^2} \frac{1}{18M} \left\{ -1 + \frac{\pi}{4} \frac{m_\pi}{M} [6 + \tau_3] \right\}, \quad (67)$$

$$\frac{1}{6M} \left\{ \frac{2}{M^2} \left(\frac{\kappa_N^2}{12} \langle r_2^2 \rangle - I_1'(0) \right) + \frac{1}{\alpha_{\text{em}}} (\gamma_{E1M2} - \gamma_{E1E1} - \delta_{LT}) \right\} = \frac{g_A^2}{(4\pi f_\pi)^2} \frac{1}{m_\pi^2} \frac{1}{9M} \times \left\{ 1 - \frac{\pi}{8} \frac{m_\pi}{M} [13 + \kappa_V + 4(1 + \kappa_S)\tau_3] \right\} \quad (68)$$

To test these predictions in HB χ PT, we need the derivatives of two GPs on the *lhs* of Eqs. (60, 61). They have been calculated at LO in the chiral expansion in Refs. [39, 40] and at NLO in Refs. [41, 42]⁴. The derivatives at $Q^2 = 0$ appearing in Eqs. (60)–(61) are given by

$$P^{(M1,M1)1}(0) = \frac{g_A^2}{(4\pi f_\pi)^2} \frac{1}{m_\pi^2} \frac{1}{18M} \left\{ -1 + \frac{\pi}{4} \frac{m_\pi}{M} [6 + \tau_3] \right\}, \quad (69)$$

$$P^{(L1,L1)1}(0) = \frac{g_A^2}{(4\pi f_\pi)^2} \frac{1}{m_\pi^2} \frac{1}{9M} \left\{ 1 - \frac{\pi}{8} \frac{m_\pi}{M} [13 + \kappa_V + 4(1 + \kappa_S)\tau_3] \right\}. \quad (70)$$

We notice that both for the GP $P^{(M1,M1)1}$ of Eq. (69) and for the GP $P^{(L1,L1)1}$ of Eq. (70) there is an exact agreement both at LO and NLO with the *rhs* of the sum rule, Eqs. (67) and (68), respectively.

⁴ Note that some algebraic errors in the original version of Ref. [42] have been corrected in the corresponding erratum listed under Ref. [42]. We also note that for the GP $P^{(L1,L1)1}$ the NLO HB χ PT result of Ref. [42] for the terms beyond the first derivative in Q^2 at $Q^2 = 0$ is incomplete as was pointed out by the recent covariant B χ PT calculation [49]. In Ref. [42], the NLO terms for the GP $P^{(L1,L1)1}$ were not calculated directly but inferred from nucleon crossing symmetry relations. As for the sum rule tests in the present work we only need the results for the first derivative $P^{(L1,L1)1}(0)$; there is an exact agreement between the corresponding terms at both LO and NLO in the B χ PT and HB χ PT results.

We can also check the leading order contribution when including Delta states by calculating the $\pi\Delta$ loop contributions in HB χ PT using the small-scale expansion (SSE) to order $\mathcal{O}(\varepsilon^3)$. The leading contributions to the spin polarizabilities and to the GPs contain terms proportional to $1/m_\pi^2$ or $1/\Delta^2$, where $\Delta = M_\Delta - M_N$. Let us introduce the dimensionless ratios:

$$\mu \equiv m_\pi/M, \quad \delta \equiv \Delta/M. \quad (71)$$

Then, denoting the leading $\pi N\Delta$ coupling constant by h_A , the Delta contributions to the various quantities which enter in the sum rules of Eqs. (60, 61) were calculated to order $\mathcal{O}(\varepsilon^3)$ in Refs. [34, 35, 40, 43, 44]:

$$P'^{(M1,M1)1}(0) \Big|_{\pi\Delta} = -\frac{h_A^2}{1296\pi^2 f_\pi^2 M M_\Delta^2} \frac{1}{\delta^2 - \mu^2} \left\{ 1 - \frac{\delta}{\sqrt{\delta^2 - \mu^2}} \ln \frac{\delta + \sqrt{\delta^2 - \mu^2}}{\mu} \right\}, \quad (72)$$

$$P'^{(L1,L1)1}(0) \Big|_{\pi\Delta} = \frac{h_A^2}{648\pi^2 f_\pi^2 M M_\Delta^2} \frac{1}{\delta^2 - \mu^2} \left\{ 1 - \frac{\delta}{\sqrt{\delta^2 - \mu^2}} \ln \frac{\delta + \sqrt{\delta^2 - \mu^2}}{\mu} \right\}, \quad (73)$$

$$\frac{1}{\alpha_{\text{em}}} \gamma_{E1,M2} \Big|_{\pi\Delta} = \frac{h_A^2}{432\pi^2 f_\pi^2 M_\Delta^2} \frac{1}{\delta^2 - \mu^2} \left\{ 1 - \frac{\delta}{\sqrt{\delta^2 - \mu^2}} \ln \frac{\delta + \sqrt{\delta^2 - \mu^2}}{\mu} \right\}, \quad (74)$$

$$\frac{1}{\alpha_{\text{em}}} \gamma_{E1,E1} \Big|_{\pi\Delta} = \frac{h_A^2}{432\pi^2 f_\pi^2 M_\Delta^2} \frac{1}{(\delta^2 - \mu^2)^2} \left\{ \delta^2 + 5\mu^2 + \frac{(\delta^2 - 7\mu^2)\delta}{\sqrt{\delta^2 - \mu^2}} \ln \frac{\delta + \sqrt{\delta^2 - \mu^2}}{\mu} \right\}, \quad (75)$$

$$\frac{1}{\alpha_{\text{em}}} \delta_{LT} \Big|_{\pi\Delta} = \frac{h_A^2}{216\pi^2 f_\pi^2 M_\Delta^2} \frac{1}{(\delta^2 - \mu^2)^2} \left\{ -2\delta^2 - \mu^2 + \frac{(\delta^2 + 2\mu^2)\delta}{\sqrt{\delta^2 - \mu^2}} \ln \frac{\delta + \sqrt{\delta^2 - \mu^2}}{\mu} \right\}, \quad (76)$$

$$I'_1(0) \Big|_{\pi\Delta} = 0, \quad (77)$$

$$\kappa_N^2 \langle r_2^2 \rangle \Big|_{\pi\Delta} = 0. \quad (78)$$

Plugging the leading order expressions of Eqs. (72-78) into the sum rules of Eqs. (60, 61), one easily verifies that both sum rules are also exactly satisfied to this order in the SSE.

IV. VERIFICATION IN COVARIANT χ PT

Using the results for the RCS spin polarizabilities and the VVCS amplitudes obtained in Refs. [45–48], as well as the results for the nucleon GPs calculated in Ref. [49], we have also verified the new sum rules in covariant B χ PT. Note that in practice it is more convenient to use the variant of the sum rules for the non-Born parts of the amplitudes S_1 and S_2 , which read

$$S_1^{\text{nb}}(\nu, Q^2) = M\gamma_0\nu^2 + MQ^2 \left\{ \gamma_{E1M2} - 3M\alpha_{\text{em}} \left[P'^{(M1,M1)1}(0) + P'^{(L1,L1)1}(0) \right] \right\} + \mathcal{O}(k^4), \quad (79)$$

$$\nu S_2^{\text{nb}}(\nu, Q^2) = -M^2\nu^2 \left\{ \gamma_0 + \gamma_{E1E1} - 3M\alpha_{\text{em}} \left[P'^{(M1,M1)1}(0) - P'^{(L1,L1)1}(0) \right] \right\} + \mathcal{O}(\nu^4, \nu^2 Q^2). \quad (80)$$

For completeness, we provide here the results for the derivatives of the two GPs in covariant B χ PT that were obtained in Ref. [49]:

1. πN loops:

a. Proton

$$\begin{aligned} P'^{(M1,M1)1}(0) \Big|_p^{\pi N} &= \frac{g_A^2}{288\pi^2 f_\pi^2 M^3} \frac{1}{\mu^2(4 - \mu^2)^{3/2}} \\ &\times \left[\mu (18\mu^8 - 143\mu^6 + 327\mu^4 - 192\mu^2 + 14) \arccos \left(\frac{\mu^2}{2} - 1 \right) \right. \\ &\quad \left. + \sqrt{4 - \mu^2} (36\mu^6 - 160\mu^4 + 98\mu^2 - 4 - (18\mu^6 - 107\mu^4 + 149\mu^2 - 36) \mu^2 \ln \mu^2) \right] \\ &= -2.3 \text{ GeV}^{-5}, \end{aligned} \quad (81)$$

$$\begin{aligned}
P'^{(L1,L1)1}(0)|_p^{\pi N} &= \frac{g_A^2}{288\pi^2 f_\pi^2 M^3} \frac{1}{\mu^2(4-\mu^2)^{5/2}} \\
&\times \left[\mu (27\mu^{10} - 321\mu^8 + 1338\mu^6 - 2250\mu^4 + 1288\mu^2 - 136) \arccos\left(\frac{\mu^2}{2} - 1\right) \right. \\
&\quad + \sqrt{4-\mu^2} \left(54\mu^8 - 453\mu^6 + 1096\mu^4 - 660\mu^2 + 32 \right. \\
&\quad \quad \left. \left. - 3(\mu^2-4)^2(9\mu^4 - 17\mu^2 + 6)\mu^2 \ln \mu^2 \right) \right] \\
&= 3.7 \text{ GeV}^{-5}.
\end{aligned} \tag{82}$$

b. Neutron

$$\begin{aligned}
P'^{(M1,M1)1}(0)|_n^{\pi N} &= \frac{g_A^2}{288\pi^2 f_\pi^2 M^3} \frac{1}{\mu^2(4-\mu^2)^{3/2}} \\
&\times \left[\mu (3\mu^4 - 18\mu^2 + 10) \arccos\left(\frac{\mu^2}{2} - 1\right) + \sqrt{4-\mu^2} (8\mu^2 - 4 - 3(\mu^2-4)\mu^2 \ln \mu^2) \right] \\
&= -2.5 \text{ GeV}^{-5},
\end{aligned} \tag{83}$$

$$\begin{aligned}
P'^{(L1,L1)1}(0)|_n^{\pi N} &= \frac{g_A^2}{144\pi^2 f_\pi^2 M^3} \frac{1}{\mu^2(4-\mu^2)^{5/2}} \\
&\times \left[3\mu (\mu^6 - 10\mu^4 + 30\mu^2 - 12) \arccos\left(\frac{\mu^2}{2} - 1\right) \right. \\
&\quad \left. + \sqrt{4-\mu^2} (7\mu^4 - 50\mu^2 + 16 - 3(\mu^2-4)^2 \mu^2 \ln \mu^2) \right] \\
&= 5.2 \text{ GeV}^{-5}.
\end{aligned} \tag{84}$$

2. $\pi\Delta$ loops:

$$\begin{aligned}
P'^{(M1,M1)1}(0)|^{\pi\Delta} &= \frac{h_A^2}{31104\pi^2 f_\pi^2 M M_\Delta^2} \\
&\times \left[-42 - 24\delta + \int_0^1 dx \left(\frac{24(1-x)x^5(1+x+\delta)}{D_\Delta(x)^2} \right. \right. \\
&\quad \left. \left. + \frac{12x^2(24x^3 - x^2(22-8\delta) - 3x(2+5\delta) + 9(1+\delta))}{D_\Delta(x)} \right. \right. \\
&\quad \left. \left. - 24x(16x^2 - x(3-9\delta) - 12(1+\delta)) [\Xi - \ln D_\Delta(x)] \right) \right] \\
&= 0.5 \text{ GeV}^{-5},
\end{aligned} \tag{85}$$

$$\begin{aligned}
P'^{(L1,L1)1}(0)|^{\pi\Delta} &= \frac{h_A^2}{31104\pi^2 f_\pi^2 M M_\Delta^2} \\
&\times \left[-16 + \int_0^1 dx \left(\frac{-24x^4(7-12x+5x^2)(1+x+\delta)}{D_\Delta(x)^2} \right. \right. \\
&\quad \left. \left. + \frac{12x^2(48x^3 - x^2(51-46\delta) - x(25+71\delta) + 24(1+\delta))}{D_\Delta(x)} \right. \right. \\
&\quad \left. \left. - 48x^2(7x-6) [\Xi - \ln D_\Delta(x)] \right) \right] \\
&= -0.8 \text{ GeV}^{-5},
\end{aligned} \tag{86}$$

with

$$D_\Delta(x) = x^2 + (1+\delta)^2 - x(2+2\delta+\delta^2-\mu^2). \tag{87}$$

The divergent parts of the polarizabilities, absorbed by higher-order contact terms, are renormalized according to the modified minimal subtraction ($\overline{\text{MS}}$) scheme, by setting to 0 the factor arising in the dimensional regularization:

$$\Xi = \frac{2}{4-D} - \gamma_E + \ln \frac{4\pi\Lambda^2}{M^2}, \quad (88)$$

with $D \simeq 4$ the number of dimensions, γ_E the Euler constant, and Λ the renormalization scale.

3. Δ -pole

$$P'^{(M1,M1)1}(0)|^{\Delta\text{-pole}} = \frac{1}{6M^2M_+^2} \left(-\frac{g_M^2}{\Delta} + 2\frac{g_M g_E}{M_+} + \frac{g_E^2}{M_+} \right) = -1.3 \text{ GeV}^{-5}, \quad (89)$$

$$P'^{(L1,L1)1}(0)|^{\Delta\text{-pole}} = \frac{1}{6M^2M_+^2} \left(-\frac{g_M g_E}{\Delta} + \frac{g_E^2}{M_+} \right) = 0.4 \text{ GeV}^{-5}, \quad (90)$$

with $M_+ = M + M_\Delta$, and where g_M (g_E) are the M1 (E2) $\gamma N\Delta$ couplings respectively [50].

We can expand the above expressions in the small scales in order to compare with the HB expressions given above. Note that these $B\chi\text{PT}$ results, namely, the answers for the πN loop contribution, do not include the photon coupling to the nucleon anomalous magnetic moment in the loop. Expanding Eqs. (81)–(84), we get

$$P'^{(M1,M1)1}(0)|_p^{\pi N} = \frac{g_A^2}{(4\pi f_\pi)^2} \frac{1}{18M^3\mu^2} \left[-1 + \frac{7\pi}{4}\mu + \left(\frac{45}{2} + 18 \ln \mu \right) \mu^2 + \dots \right], \quad (91)$$

$$P'^{(L1,L1)1}(0)|_p^{\pi N} = \frac{g_A^2}{(4\pi f_\pi)^2} \frac{1}{9M^3\mu^2} \left[1 - \frac{17\pi}{8}\mu - 18(1 + \ln \mu) \mu^2 + \dots \right], \quad (92)$$

$$P'^{(M1,M1)1}(0)|_n^{\pi N} = \frac{g_A^2}{(4\pi f_\pi)^2} \frac{1}{18M^3\mu^2} \left[-1 + \frac{5\pi}{4}\mu + \left(\frac{1}{2} + 6 \ln \mu \right) \mu^2 + \dots \right], \quad (93)$$

$$P'^{(L1,L1)1}(0)|_n^{\pi N} = \frac{g_A^2}{(4\pi f_\pi)^2} \frac{1}{9M^3\mu^2} \left[1 - \frac{9\pi}{8}\mu - \left(\frac{3}{2} + 6 \ln \mu \right) \mu^2 + \dots \right], \quad (94)$$

which coincides up to the NLO with the result of Eqs. (69)–(70) if one sets $\kappa_S = \kappa_V = 0$.

The $\pi\Delta$ loop contributions can be expanded in the small quantities δ and μ by, e.g., substituting $\delta \rightarrow \eta\delta$, $\mu \rightarrow \eta\mu$ into Eqs. (85) and (86), integrating over the Feynman parameter x , expanding the result in powers of η and setting $\eta = 1$ in the end. This results in

$$P'^{(M1,M1)1}(0)|^{\pi\Delta} = \frac{h_A^2}{1296\pi^2 f_\pi^2 M M_\Delta^2} \frac{1}{(\delta^2 - \mu^2)} \times \left[-1 + \frac{\delta}{\sqrt{\delta^2 - \mu^2}} \ln \frac{\delta + \sqrt{\delta^2 - \mu^2}}{\mu} - \frac{9}{2}\delta + \frac{4\delta^2 + 5\mu^2}{2\sqrt{\delta^2 - \mu^2}} \ln \frac{\delta + \sqrt{\delta^2 - \mu^2}}{\mu} + \dots \right], \quad (95)$$

$$P'^{(L1,L1)1}(0)|^{\pi\Delta} = \frac{h_A^2}{648\pi^2 f_\pi^2 M M_\Delta^2} \frac{1}{(\delta^2 - \mu^2)} \times \left[1 - \frac{\delta}{\sqrt{\delta^2 - \mu^2}} \ln \frac{\delta + \sqrt{\delta^2 - \mu^2}}{\mu} + \delta - \frac{\delta^2 + \mu^2}{2\sqrt{\delta^2 - \mu^2}} \ln \frac{\delta + \sqrt{\delta^2 - \mu^2}}{\mu} + \dots \right], \quad (96)$$

whose LO coincides with the LO HB χPT results of Eqs. (72-73).

V. EMPIRICAL VERIFICATION

In the following, we will investigate the empirical verification of the sum rules for $I'_1(0)$ as well as for δ_{LT} . The *rhs* of the sum rule of Eq. (46) requires the information for the Pauli radius and phenomenological dispersive estimates for the spin and generalized spin polarizabilities. To evaluate the Pauli radius, we can

use the experimental information on the electric $\langle r_E^2 \rangle$ and magnetic $\langle r_M^2 \rangle$ radii of the nucleon. The Pauli radius is obtained from those quantities as

$$\kappa_N \langle r_2^2 \rangle = \mu_N \langle r_M^2 \rangle - \langle r_E^2 \rangle + \frac{3\kappa_N}{2M^2}, \quad (97)$$

where μ_N denotes the nucleon magnetic moment. Using the recent experimental values for the proton electric and magnetic radii from Ref. [51],

$$\begin{aligned} \langle r_E^2 \rangle &= 0.77 \pm 0.01 \text{ fm}^2, \\ \langle r_M^2 \rangle &= 0.60 \pm 0.03 \text{ fm}^2, \end{aligned} \quad (98)$$

one obtains for the proton Pauli radius

$$\langle r_2^2 \rangle = 0.58 \pm 0.04 \text{ fm}^2. \quad (99)$$

We next turn to the spin polarizability contributions to both sum rules of Eqs. (46) and (59). These spin polarizabilities contain in general a π^0 -pole contribution and a non-pole contribution. The latter can be evaluated by an unsubtracted dispersion relation. The π^0 -pole contribution to the relevant spin polarizabilities and to the slopes of the spin GPs entering the sum rule are given by

$$\begin{aligned} \frac{1}{\alpha_{\text{em}}} \gamma_{E1M2} |^{\pi^0} &= \frac{1}{2} C_\pi, & \frac{1}{\alpha_{\text{em}}} \gamma_{E1E1} |^{\pi^0} &= \frac{1}{2} C_\pi, \\ P'^{(M1,M1)1}(0) |^{\pi^0} &= \frac{1}{6M} C_\pi, & P'^{(L1,L1)1}(0) |^{\pi^0} &= 0, \end{aligned} \quad (100)$$

with $C_\pi = g_A/(4\pi^2 f_\pi^2 m_\pi^2)$. By inserting these into the sum rules of Eqs. (46) and (59), one notices that the π^0 -pole contribution drops out of the *rhs* of both sum rules. This is consistent, as the *lhs* of these sum rules, corresponding with the moments of g_1 and g_2 , do not contain such π^0 -pole contributions.

The non-pole parts of the spin polarizabilities have been estimated phenomenologically using unsubtracted dispersion relations [5, 52]. The corresponding dispersive estimates for the generalized polarizabilities have been performed in Refs. [5, 53]. To show the uncertainty due to the phenomenological input in the dispersion relations, we show in Table I the dispersive results for the spin and generalized spin polarizabilities using either MAID2000 [54] or MAID2007 [55] as input for the πN channel contribution.

Very recently, a first experimental extraction of the four proton spin polarizabilities was performed using polarized Compton scattering on a proton target, resulting in the values [56]

$$\gamma_{E1M2} = (-0.7 \pm 1.2) \times 10^{-4} \text{ fm}^4, \quad (101)$$

$$\gamma_{E1E1} = (-3.5 \pm 1.2) \times 10^{-4} \text{ fm}^4. \quad (102)$$

We like to notice that the above values result from a fit of the four proton dipole spin polarizabilities to one double polarization Compton scattering observable, one single polarization observable (photon asymmetry), the backward spin polarizability combination γ_π , extracted from unpolarized experiments, as well as the forward spin polarizability combination γ_0 . The large error of γ_{E1M2} which results from the fit in Ref. [56] is mainly due to the present large error on γ_π , given by $\delta\gamma_\pi = 1.8 \times 10^{-4} \text{ fm}^4$. Ongoing measurements of another double polarization Compton scattering observable will allow one to reduce the error on γ_π by a factor of 4, which is expected to reduce the error on the other spin polarizabilities accordingly.

Based on the above experimental and phenomenological values, we compare in Table I the different contributions to the proton generalized GDH sum rule of Eq. (46) as well as the sum rule of Eq. (59) for δ_{LT} . For the sum rule of Eq. (46), we can compare this result directly with the experimental value for $I'_1(0)$ as measured by JLab/CLAS [57]. We see that within the error bars, the phenomenological DR estimate for the proton sum rule (SR) value of $I'_1(0)$ is in good agreement with the experimental value. For the sum rule of Eq. (59), the experimental value of δ_{LT} is not yet available. Comparing with the phenomenological estimate of Ref. [11], one finds an agreement of this sum rule within 10%; see the last row in Table I. A recent JLab experiment to measure δ_{LT} , which is currently under analysis, will allow one to provide a direct experimental verification of the sum rule of Eq. (59) in the near future.

We provide a graphical presentation of both spin-dependent sum rules in Figs. 1 and 2. Using only the empirical information for $I'_1(0)$ and δ_{LT} , the sum rules provide a slanted (brown) band in the plots of

	Disp. rel. MAID2000	Disp. rel. MAID2007	HB χ PT πN to $\mathcal{O}(p^4)$	B χ PT πN	B χ PT $\pi N + \Delta + \pi\Delta$	Experiment
γ_{E1M2} [10^{-4} fm^4]	-0.03 [52]	-0.1 [5, 55]	0.2 [38]	0.5 [48]	0.2 ± 0.2 [48]	-0.7 ± 1.2 [56]
γ_{E1E1} [10^{-4} fm^4]	-4.3 [52]	-4.3 [5, 55]	-1.3 [38]	-3.4 [48]	-3.3 ± 0.8 [48]	-3.5 ± 1.2 [56]
$P'^{(M1,M1)1}(0)$ [GeV^{-5}]	-5.8 [53, 54]	-4.7 [53, 55]	-0.7 [41, 42]	-2.3	-3.0 ± 0.7 [49]	–
$P'^{(L1,L1)1}(0)$ [GeV^{-5}]	3.4 [53, 54]	4.3 [53, 55]	-1.3 [41, 42]	3.7	3.4 ± 0.9 [49]	–
$\langle r_2^2 \rangle$ [fm^2]			0.55 [37]	–	–	0.58 ± 0.04 [51]
$I'_1(0)$ [GeV^{-2}]	6.8 (SR)	4.0 (SR)	7.1 [10, 36]	–	–	7.6 ± 2.5 [57]
$I'_1(0) - \frac{\kappa_N^2}{12} \langle r_2^2 \rangle$ [GeV^{-2}]	2.9 (SR)	0.1 (SR)	3.3 [10, 36]	0.3	0.3 ± 0.1 [46]	2.6 ± 2.5 [57]
δ_{LT} [10^{-4} fm^4]	1.5 (SR)	1.5 (SR)	1.5 [34]	1.5	1.4 ± 0.3 [46]	1.34 [11, 55] (MAID2007)

TABLE I: Estimates for the different quantities which enter the generalized GDH sum rule of Eq. (46) and the sum rule for δ_{LT} of Eq. (59) for the proton. The first and second data columns show the dispersive estimates (Disp. rel.) using respectively MAID2000 [54] and MAID2007 [55] as input for the (generalized) spin polarizabilities. Third data column: HB χ PT results to $\mathcal{O}(p^4)$. Fourth data column: πN loop results within covariant B χ PT. Fifth data column: πN loop + Δ -pole + $\pi\Delta$ loop results within covariant B χ PT (with errors calculated as explained in Ref. [48]). The last column shows the experimental values. The values for $I'_1(0)$ and δ_{LT} show the corresponding SR estimates, based on Eqs. (46) and (59) respectively. We also show the result for the quantity $I'_1(0) - \frac{\kappa_N^2}{12} \langle r_2^2 \rangle$, which is predictable in B χ PT.

γ_{E1M2} and γ_{E1E1} versus the slopes of the GPs. The pioneering experimental values for γ 's, recently obtained by the A2 Collaboration at MAMI [56], are shown by the broad horizontal (yellow) band in the figures. The region where the two bands overlap yields a prediction for the slopes of the GPs. A measurement of GP slopes using VCS is required to directly verify this prediction. One sees from both figures that the phenomenological DR estimates of Pasquini *et al.* [5] (shown by the horizontal and vertical purple bands) are well in agreement, within uncertainties, with the RCS spin polarizabilities and are consistent with the sum rule bands. The figures also show the results obtained in the covariant B χ PT ($\pi N + \Delta + \pi\Delta$). We have checked above that both the covariant and HB χ PT calculations satisfy the sum rules exactly. Within the present error bars, the B χ PT results are in agreement with the RCS spin polarizabilities [the same is also true for the HB χ PT calculation (not shown in the figures), although for γ_{E1E1} the HB χ PT extraction yields a large uncertainty [58]]. The B χ PT results for the slopes of the two spin GPs are also in good agreement with the DR estimates, as noted in Ref. [49].

In Fig. 3, we provide an alternative presentation of the sum rule of Eq. (59) by presenting γ_{E1E1} versus δ_{LT} . The value of the spin GP combination ($P'^{(M1,M1)1}(0) - P'^{(L1,L1)1}(0)$) is taken from the DR estimate, yielding the slanted (purple) sum rule band. For the spin polarizabilities, we have presented two variants of covariant B χ PT: the results of Lensky *et al.* [46, 48] shown in Table I, and the results of Bernard *et al.* [59]. They are done in two different counting schemes for the Δ -isobar contribution. One notices that they yield a noticeable difference in the value for δ_{LT} which is mainly due to a much larger contribution of the $\pi\Delta$ loops in Ref. [59] as compared to Ref. [46]. One notices that the phenomenological MAID estimate [11, 55] for δ_{LT} favors the smaller value for δ_{LT} of both B χ PT variants. The recent JLab proton δ_{LT} experiment, which is currently under analysis, will allow a direct experimental verification of this puzzle.

VI. PREDICTIONS FOR THE VCS RESPONSE FUNCTION P_{TT} AT LOW Q^2

One combination of the VCS spin polarizabilities can be obtained in an unpolarized VCS experiment. At low energy (q') of the emitted photon, the energy dependence of the $ep \rightarrow ep\gamma$ unpolarized cross section

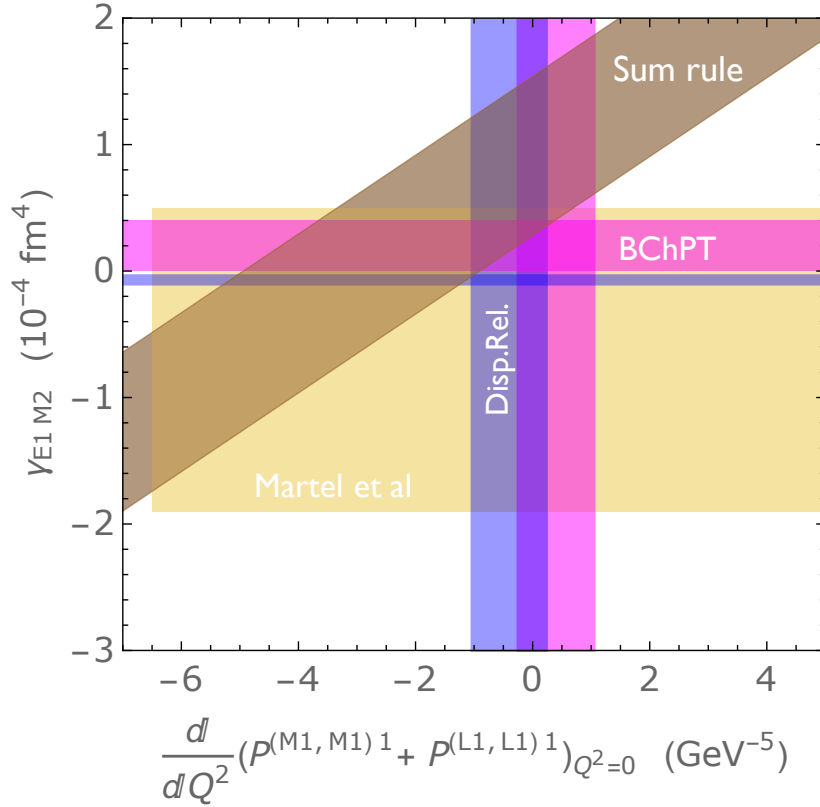


FIG. 1: The sum rule relation of Eq. (46) between γ_{E1M2} versus $(P^{(M1,M1)1}(0) + P^{(L1,L1)1}(0))$. The brown band is the sum rule constraint based on the empirical information for $I_1'(0)$ from [57], and for $\langle r_2^2 \rangle$ from [51]. The yellow band is the empirical extraction of γ_{E1M2} from [56]. The purple bands are the DR evaluations [5] for the RCS and VCS polarizabilities, where the width of the bands is obtained by using either MAID2000 [54] or MAID2007 [55] as input in the dispersive evaluations. The pink bands are the $B_\chi\text{PT}$ evaluations ($\pi N + \Delta + \pi\Delta$ results from Table I) [46, 48, 49].

can be expressed through a Taylor expansion in q' , taking the lowest three terms into account. In such an expansion in q' , the experimentally extracted VCS unpolarized squared amplitude \mathcal{M}^{exp} takes the form [15]

$$\mathcal{M}^{\text{exp}} = \frac{\mathcal{M}_{-2}^{\text{exp}}}{q'^2} + \frac{\mathcal{M}_{-1}^{\text{exp}}}{q'} + \mathcal{M}_0^{\text{exp}} + O(q'). \quad (103)$$

Due to the low-energy theorem (LET), the threshold coefficients $\mathcal{M}_{-2}^{\text{exp}}$ and $\mathcal{M}_{-1}^{\text{exp}}$ are known [15], and are fully determined from the Bethe-Heitler + Born (BH + Born) amplitudes. The information on the GPs is contained in $\mathcal{M}_0^{\text{exp}}$, which contains a part originating from the BH+Born amplitudes and another one which is a linear combination of the GPs, with coefficients determined by the kinematics. The unpolarized observable $\mathcal{M}_0^{\text{exp}}$ can be expressed in terms of three structure functions $P_{LL}(Q^2)$, $P_{TT}(Q^2)$, and $P_{LT}(Q^2)$ by [15]

$$\mathcal{M}_0^{\text{exp}} - \mathcal{M}_0^{\text{BH+Born}} = 2K \left\{ v_1 [\varepsilon P_{LL}(Q^2) - P_{TT}(Q^2)] + \left(v_2 + \sqrt{\frac{\tau}{1+\tau}} v_3 \right) \sqrt{2\varepsilon(1+\varepsilon)} P_{LT}(Q^2) \right\}, \quad (104)$$

where K is a kinematical factor, ε is the virtual photon polarization (in the standard notation used in electron scattering), and v_1, v_2, v_3 are kinematical quantities depending on ε and Q^2 as well as on the c.m. polar and azimuthal angles of the produced real photon (for details see Ref. [16]). The three unpolarized observables of Eq. (104) can be expressed in terms of the six GPs as [15, 16]

$$P_{LL} = -2\sqrt{6} M G_E P^{(L1,L1)0}, \quad (105)$$

$$P_{TT} = 6M G_M (1 + \tau) \left[2\sqrt{2} M \tau P^{(L1,M2)1} + P^{(M1,M1)1} \right], \quad (106)$$

$$P_{LT} = \sqrt{\frac{3}{2}} M \sqrt{1 + \tau} \left[G_E P^{(M1,M1)0} - \sqrt{6} G_M P^{(L1,L1)1} \right], \quad (107)$$

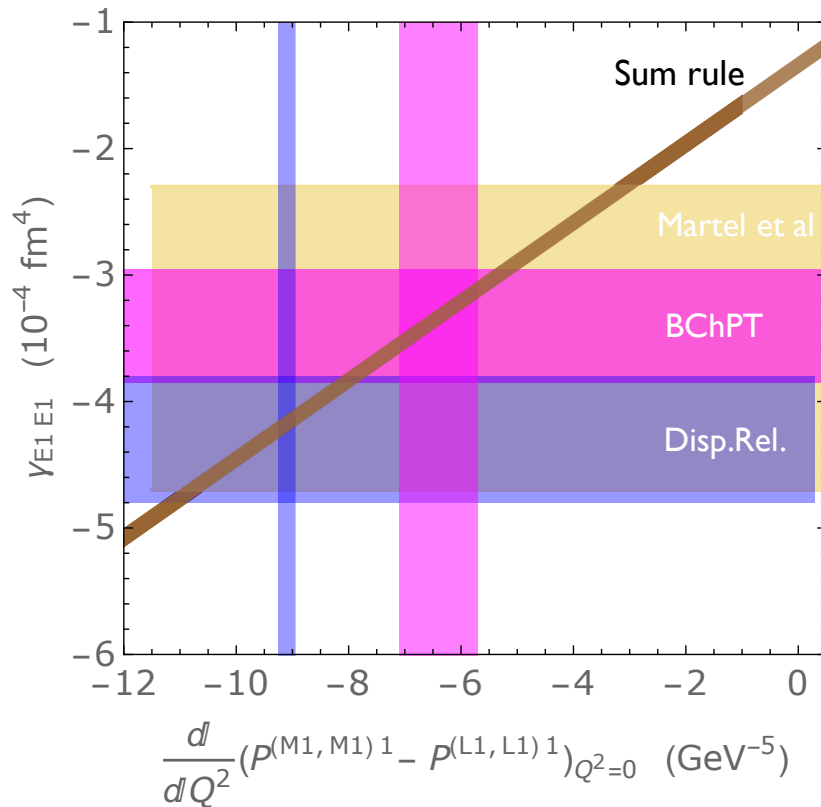


FIG. 2: The sum rule relation of Eq. (59) between γ_{E1E1} versus $(P^{(M1, M1)1}(0) - P^{(L1, L1)1}(0))$. The brown band is the sum rule constraint based on the phenomenological MAID2007 [55] information for δ_{LT} . The yellow band is the empirical extraction of γ_{E1E1} from [56]. The purple bands are the DR evaluations [5] for the RCS and VCS polarizabilities, where the width of the bands is obtained by using either MAID2000 [54] or MAID2007 [55] as input in the dispersive evaluations. The pink bands are the $B\chi$ PT evaluations ($\pi N + \Delta + \pi\Delta$ results from Table I) [46, 48, 49].

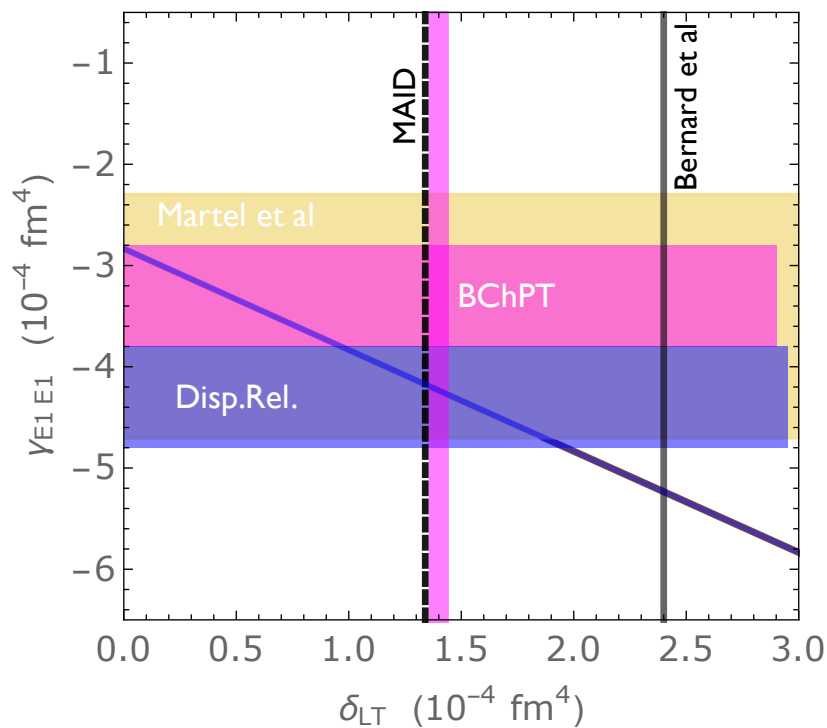


FIG. 3: Spin polarizabilities, γ_{E1E1} versus δ_{LT} , for the proton. Results for γ_{E1E1} (horizontal bands) are from: the experiment of [56] (yellow), the $B\chi$ PT calculation of [48] (red), and the fixed- t DR calculation of [5, 52] (purple). Results for δ_{LT} (vertical bands) are from: MAID2007 [11, 55] (dashed line), [46] (pink), and [59] (gray). The line across is based on the sum rule using the values of GPs from the DR calculation of [53].

where the nucleon form factors $G_E \equiv F_D + \tau F_P$ and G_M depend on Q^2 .

We notice from Eq. (106) that the VCS response function P_{TT} involves only spin GPs and vanishes at $Q^2 = 0$. The slope at $Q^2 = 0$ of P_{TT} can be expressed as

$$\begin{aligned} P'_{TT}(0) &\equiv \left. \frac{d}{dQ^2} P_{TT}(Q^2) \right|_{Q^2=0} \\ &= 2\mu_N \left\{ 3MP'^{(M1,M1)1}(0) - \frac{1}{\alpha_{\text{em}}} \gamma_{E1M2} \right\} \\ &= 2\mu_N \left\{ \frac{1}{M^2} \left(\frac{\kappa_N^2}{12} \langle r_2^2 \rangle - I'_1(0) \right) + \frac{1}{2\alpha_{\text{em}}} (-\gamma_{E1M2} + \gamma_{E1E1} + \delta_{LT}) \right\}, \end{aligned} \quad (108)$$

with μ_N the nucleon magnetic moment, and where the last line has been obtained by eliminating $P'^{(M1,M1)1}(0)$ by using the sum rules of Eqs. (46) and (59).

When plugging the respective values into the last line of Eq. (108), by using the values listed in Table I, we obtain the DR prediction, the respective χ PT predictions, as well as the empirical prediction for the slope at $Q^2 = 0$ of P_{TT} , which we list in Table II.

	Disp. rel. MAID2000	Disp. rel. MAID2007	HB χ PT πN to $\mathcal{O}(p^4)$	B χ PT πN	B χ PT $\pi N + \Delta + \pi\Delta$	Empirical SR evaluation
$P'_{TT}(0)$ [GeV $^{-4}$]	-88	-68	-21	-63	-60 ± 10	-53 ± 46

TABLE II: Different estimates for the VCS response function $P'_{TT}(0)$.

In Fig. 4, we show the predictions of the DR and chiral calculations for P_{TT}/Q^2 at low $Q^2 \leq 0.1$ GeV 2 , together with the empirical evaluation at $Q^2 = 0$. One can again see that the DR and B χ PT predictions agree quite well, whereas the HB χ PT curve is much smaller. All these theoretical calculations are compatible with the result of the empirical evaluation within the present sizable uncertainty of the latter.

VII. SUMMARY AND CONCLUSION

By generalizing the Gerasimov-Drell-Hearn sum rule to finite photon virtuality, we obtain the two new model-independent relations. They link the parameters characterizing different sectors of low-energy interactions between the nucleon spin structure and electromagnetic waves. The parameters, involved in these relations, are extracted from experimental information on nucleon Compton scattering in different regimes: RCS (spin polarizabilities), VCS (generalized polarizabilities), and VVCS (longitudinal-transverse polarizability and the generalized GDH integral). In addition, they involve the nucleon form factors in the form of the Pauli radii and the anomalous magnetic moments.

These relations are identically verified in B χ PT and in HB χ PT. We have also studied their empirical consequences, and found that the current experimental extractions and phenomenological estimates done in the fixed- t DR framework for the proton are consistent with the sum rules. The B χ PT predictions are also in agreement with these relations (with the notable exception of the δ_{LT} where there appears to be a disagreement between the B χ PT calculations of Ref. [46] and Ref. [59]). We have used the relations to evaluate the slope of the VCS response function P_{TT} at zero virtuality and compared it with the results of the DR and of the chiral calculations. The covariant B χ PT and the DR give similar results for $P'_{TT}(0)$, whereas the HB χ PT value is considerably different from them. The empirical result, obtained using the new relation has yet a large uncertainty, but in the future will be able to discriminate between the predictions.

The new relations have thus been shown to hold in a quantum-field-theoretic framework and are proving to be useful in constraining the low-energy spin structure of the nucleon.

Acknowledgments

We would like to thank Barbara Pasquini for helpful discussions. This work was supported by the Deutsche Forschungsgemeinschaft (DFG) in part through the Collaborative Research Center [The Low-

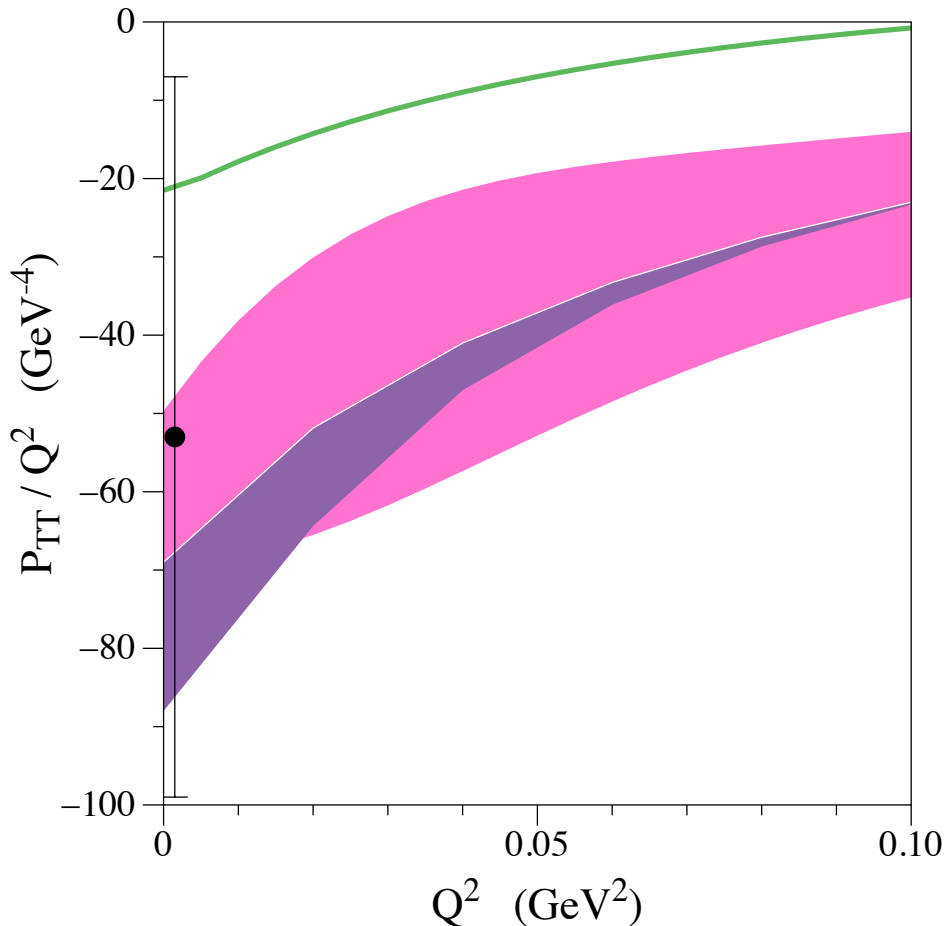


FIG. 4: Q^2 dependence of the VCS response function P_{TT}/Q^2 . The purple band is the DR estimate [5] where the width of the band corresponds to the evaluations obtained by using MAID2007 [55] (upper) or MAID2000 [54] (lower). The green curve is the NLO prediction of HB χ PT, corresponding with πN loops to $\mathcal{O}(p^4)$. The red band at low Q^2 is the B χ PT prediction ($\pi N + \Delta + \pi\Delta$) of Ref. [49]. The data point at $Q^2 = 0$ corresponds with the empirical sum rule evaluation according to the last column in Table II.

Energy Frontier of the Standard Model (SFB 1044)], and in part through the Cluster of Excellence [Precision Physics, Fundamental Interactions and Structure of Matter (PRISMA)], and by the Ministry of Science and Technology of Taiwan under Grants NSC 102-2112-M-033-005-MY3 and MOST 105-2112-M-033-004.

-
- [1] M. Gell-Mann, M. L. Goldberger and W. E. Thirring, Phys. Rev. **95**, 1612 (1954).
 - [2] S. B. Gerasimov, Sov. J. Nucl. Phys. **2**, 430 (1966) [Yad. Fiz. **2**, 598 (1965)].
 - [3] S. D. Drell and A. C. Hearn, Phys. Rev. Lett. **16**, 908 (1966).
 - [4] A. M. Baldin, Nucl. Phys. **18**, 310 (1960).
 - [5] D. Drechsel, B. Pasquini and M. Vanderhaeghen, Phys. Rept. **378**, 99 (2003).
 - [6] M. Schumacher, Prog. Part. Nucl. Phys. **55**, 567 (2005).
 - [7] H. W. Griesshammer, J. A. McGovern, D. R. Phillips and G. Feldman, Prog. Part. Nucl. Phys. **67**, 841 (2012).
 - [8] F. Hagelstein, R. Miskimen and V. Pascalutsa, Prog. Part. Nucl. Phys. **88**, 29 (2016).
 - [9] M. Anselmino, B. L. Ioffe and E. Leader, Sov. J. Nucl. Phys. **49**, 136 (1989) [Yad. Fiz. **49**, 214 (1989)].
 - [10] X.-D. Ji and J. Osborne, J. Phys. G **27**, 127 (2001).
 - [11] D. Drechsel, S. S. Kamalov and L. Tiator, Phys. Rev. D **63**, 114010 (2001)
 - [12] D. Drechsel and L. Tiator, Ann. Rev. Nucl. Part. Sci. **54**, 69 (2004).
 - [13] S. E. Kuhn, J.-P. Chen and E. Leader, Prog. Part. Nucl. Phys. **63**, 1 (2009).
 - [14] J. P. Chen, Int. J. Mod. Phys. E **19**, 1893 (2010).
 - [15] P. A. M. Guichon, G. Q. Liu and A. W. Thomas, Nucl. Phys. A **591**, 606 (1995).

- [16] P. A. M. Guichon and M. Vanderhaeghen, *Prog. Part. Nucl. Phys.* **41**, 125 (1998).
- [17] M. Gorchtein, C. Lorcé, B. Pasquini and M. Vanderhaeghen, *Phys. Rev. Lett.* **104**, 112001 (2010).
- [18] J. Roche *et al.* [VCS and A1 Collaborations], *Phys. Rev. Lett.* **85**, 708 (2000).
- [19] P. Janssens *et al.* [A1 Collaboration], *Eur. Phys. J. A* **37**, 1 (2008).
- [20] N. d'Hose, *Eur. Phys. J. A* **28S1**, 117 (2006).
- [21] L. Doria *et al.* [A1 Collaboration], *Phys. Rev. C* **92**, 054307 (2015).
- [22] L. Correa, PhD Thesis, Johannes Gutenberg-Universität, Mainz and Université Blaise Pascal, Clermont-Ferrand (2016).
- [23] P. Bourgeois *et al.*, *Phys. Rev. Lett.* **97**, 212001 (2006).
- [24] P. Bourgeois *et al.*, *Phys. Rev. C* **84**, 035206 (2011).
- [25] G. Laveissiere *et al.* [Jefferson Lab Hall A Collaboration], *Phys. Rev. Lett.* **93**, 122001 (2004).
- [26] H. Fonvieille *et al.* [Jefferson Lab Hall A Collaboration], *Phys. Rev. C* **86**, 015210 (2012).
- [27] V. Pascalutsa and M. Vanderhaeghen, *Phys. Rev. D* **91**, 051503 (2015).
- [28] D. Drechsel, G. Knöchlein, A. Yu. Korchin, A. Metz, and S. Scherer, *Phys. Rev. C* **57**, 941 (1998); *ibid.* **58**, 1751 (1998).
- [29] R. Tarrach, *Nuovo Cim. A* **28**, 409 (1975).
- [30] J. Bernabeu and R. Tarrach, *Annals Phys.* **102**, 323 (1976).
- [31] H. Burkhardt and W. N. Cottingham, *Annals Phys.* **56**, 453 (1970).
- [32] W.-Y. Tsai, L.L. DeRaad Jr, K. A. Milton, *Phys. Rev. D* **11**, 3537 (1975).
- [33] G. Altarelli, B. Lampe, P. Nason, G. Ridolfi, *Phys. Lett. B* **334**, 187 (1994).
- [34] C. W. Kao, T. Spitzenberg and M. Vanderhaeghen, *Phys. Rev. D* **67**, 016001 (2003).
- [35] C.-W. Kao, D. Drechsel, S. Kamalov and M. Vanderhaeghen, *Phys. Rev. D* **69**, 056004 (2004).
- [36] X.-D. Ji, C.-W. Kao and J. Osborne, *Phys. Lett. B* **472**, 1 (2000).
- [37] V. Bernard, N. Kaiser, and U.-G. Meissner, *Int. J. Mod. Phys. E* **4**, 193 (1995).
- [38] K. B. Vijaya Kumar, J. A. McGovern and M. C. Birse, *Phys. Lett. B* **479**, 167 (2000).
- [39] T. R. Hemmert, B. R. Holstein, G. Knöchlein, and S. Scherer, *Phys. Rev. Lett.* **79**, 22 (1997); *Phys. Rev. D* **55**, 2630 (1997).
- [40] T. R. Hemmert, B. R. Holstein, G. Knochlein and D. Drechsel, *Phys. Rev. D* **62**, 014013 (2000).
- [41] C. W. Kao and M. Vanderhaeghen, *Phys. Rev. Lett.* **89**, 272002 (2002).
- [42] C.-W. Kao, B. Pasquini and M. Vanderhaeghen, *Phys. Rev. D* **70**, 114004 (2004); Erratum: [*Phys. Rev. D* **92**, 119906 (2015)].
- [43] T. R. Hemmert, B. R. Holstein, J. Kambor and G. Knochlein, *Phys. Rev. D* **57**, 5746 (1998).
- [44] M. Gockeler *et al.* [QCDSF Collaboration], *Phys. Rev. D* **71**, 034508 (2005).
- [45] V. Lensky and V. Pascalutsa, *Eur. Phys. J. C* **65**, 195 (2010).
- [46] V. Lensky, J. M. Alarcón and V. Pascalutsa, *Phys. Rev. C* **90**, 055202 (2014).
- [47] V. Lensky and J. A. McGovern, *Phys. Rev. C* **89**, 032202 (2014).
- [48] V. Lensky, J. McGovern and V. Pascalutsa, *Eur. Phys. J. C* **75**, 604 (2015).
- [49] V. Lensky, V. Pascalutsa and M. Vanderhaeghen, *Eur. Phys. J. C* **77**, 119 (2017).
- [50] V. Pascalutsa, M. Vanderhaeghen and S. N. Yang, *Phys. Rept.* **437**, 125 (2007).
- [51] J. C. Bernauer *et al.* [A1 Collaboration], *Phys. Rev. C* **90**, 015206 (2014).
- [52] B. R. Holstein, D. Drechsel, B. Pasquini and M. Vanderhaeghen, *Phys. Rev. C* **61**, 034316 (2000).
- [53] B. Pasquini, M. Gorchtein, D. Drechsel, A. Metz and M. Vanderhaeghen, *Eur. Phys. J. A* **11**, 185 (2001).
- [54] D. Drechsel, O. Hanstein, S. S. Kamalov and L. Tiator, *Nucl. Phys. A* **645**, 145 (1999).
- [55] D. Drechsel, S. S. Kamalov and L. Tiator, *Eur. Phys. J. A* **34**, 69 (2007).
- [56] P. P. Martel *et al.* [A2 Collaboration], *Phys. Rev. Lett.* **114**, 112501 (2015).
- [57] Y. Prok *et al.* [CLAS Collaboration], *Phys. Lett. B* **672**, 12 (2009).
- [58] H. W. Griesshammer, J. A. McGovern and D. R. Phillips, *Eur. Phys. J. A* **52**, 139 (2016)
- [59] V. Bernard, E. Epelbaum, H. Krebs and U.-G. Meissner, *Phys. Rev. D* **87**, 054032 (2013).